

## 2018 MARS INSIGHT MISSION DESIGN AND NAVIGATION OVERVIEW

**Fernando Abilleira<sup>\*</sup>, Allen Halsell<sup>†</sup>, Min-Kun Chung<sup>‡</sup>, Ken Fujii<sup>§</sup>,  
Eric Gustafson<sup>\*\*</sup>, Yungsun Hahn<sup>††</sup>, Julim Lee<sup>‡‡</sup>,  
Sarah Elizabeth McCandless<sup>§§</sup>, Neil Mottinger<sup>\*\*\*</sup>, Jill Seubert<sup>†††</sup>,  
Evgeniy Sklyanskiy<sup>‡‡‡</sup>, Mark Wallace<sup>§§§</sup>**

Originally scheduled for a launch in the 2016 Earth to Mars opportunity, NASA's Interior Exploration using Seismic Investigations, Geodesy, and Heat Transport (InSight) mission will launch the next lander to Mars in May-June 2018 arriving to the Red Planet in November 2018. Derived from the Phoenix mission which successfully landed on Mars in May 2008, the InSight Entry, Descent, and Landing system will place a lander in the Elysium Planitia region. This paper specifies the mission and navigation requirements set by the Project and how the final mission and navigation design satisfies those requirements.

### INTRODUCTION

The Interior Exploration using Seismic Investigations, Geodesy, and Heat Transport (InSight) Mission has the primary objective of placing a science lander on the surface of Mars followed by the deployment of two science instruments onto the Martian surface to investigate the fundamental processes of terrestrial planet formation and evolution. By performing the first comprehensive surface-based geophysical investigation of Mars, InSight will provide key information on the composition and structure of an Earth-like planet that has gone through most of the evolutionary stages of the Earth up to, but not including, plate tectonics. The InSight launch in 2016 was suspended due to critical issues with the Seismic Experiment for Interior Structure (SEIS) instrument that could not be fixed prior to the planned launch period.

The primary systems for the InSight project are the Flight System, the Mission System, the launch vehicle, and the ground stations of the Deep Space Network (DSN). The Phoenix-heritage flight system consists of the cruise stage, the entry system, and the lander. The entry system consists of the backshell, parachute, and heat shield. The InSight mission will deliver the InSight lander to the surface of Mars in the 2018 Earth-Mars opportunity. The InSight spacecraft will be launched in May-June 2018 from Vandenberg

---

\* InSight Deputy Mission Design & Navigation Manager, Fernando.Abilleira@jpl.nasa.gov

† InSight Mission Design & Navigation Manager / Navigation Team Chief, Charles.A.Halsell@jpl.nasa.gov

‡ InSight Maneuver Analyst, Min-Kun.Chung@jpl.nasa.gov

§ InSight Mission Engineer, Kenneth.K.Fujii@jpl.nasa.gov

\*\* InSight Orbit Determination Lead, Eric.D.Gustafson@jpl.nasa.gov

†† InSight Maneuver Analyst, Yungsun.Hahn@jpl.nasa.gov

‡‡ InSight Orbit Determination Analyst, Julim.Lee@jpl.nasa.gov

§§ InSight Orbit Determination Analyst, Sarah.E.McCandless@jpl.nasa.gov

\*\*\* InSight Orbit Determination Analyst, Neil.Mottinger@jpl.nasa.gov

††† InSight Orbit Determination Analyst, Jill.Tombasco@jpl.nasa.gov

‡‡‡ InSight Entry, Descent, and Landing Trajectory Analyst, Evgeniy.Sklyanskiy@jpl.nasa.gov

§§§ InSight Trajectory Lead, Mark.S.Wallace@jpl.nasa.gov

Jet Propulsion Laboratory, California Institute of Technology, 4800 Oak Grove Drive, Pasadena, CA 91109

Air Force Base (VAFB) in California on a United Launch Alliance (ULA) Atlas V 401 and will arrive at Mars in November 2018.

## MISSION

### Launch

InSight will be launched onto a ballistic, Type 1 trajectory using an Atlas V 401 launch vehicle (LV) from Space Launch Complex 3E (SLC-3E) at VAFB in California. The 35-day launch period extends from May 5 through June 8, 2018. The launch flight azimuth is maintained constant at 158 deg across the launch period and is designed to avoid a flight over the Channel Islands. The Centaur first burn, which is the longer of the two Centaur upper stage firings, will inject the vehicle into a ~185 km circular park orbit inclined at 64 deg. After coasting for 59 to 66 min, the Centaur/spacecraft stack will reach the proper position for the second Centaur burn to inject the spacecraft onto the desired departure trajectory. The launch window on any given day during the launch period has a duration between 115 and 120 min. Launch windows are typically determined by launch vehicle performance and the required injection energy, but for InSight, shorter launch windows are constrained by estimated injection errors. The launch vehicle injection targets are specified as twice the hyperbolic injection energy per unit mass (C3), declination of the launch asymptote (DLA), and right ascension of the launch asymptote (RLA) at the Targeting Interface Point (TIP), defined as Main Engine Cutoff #2 (MECO2) plus 20 min. The injected spacecraft mass is 700.5 kg. Propellant Margin (PM) defined as the additional burnable propellant beyond the Flight Performance Reserve (FPR), and Launch Vehicle Contingency (LVC), is used to create daily launch windows. In addition to the InSight spacecraft, two secondary technology demonstration payloads known as the Mars Cubesat One (MarCO) –A and –B will be launched with InSight. The MarCO spacecraft will provide a real-time telemetry link between the InSight spacecraft and Earth during InSight’s Entry, Descent and Landing (EDL) phase at Mars.

### Interplanetary Cruise

During the 6.5-month interplanetary flight of the spacecraft, up to six planned trajectory correction maneuvers (TCMs) will be employed to remove the planetary protection-required aimpoint bias, correct any launch vehicle injection errors, and deliver InSight to its intended entry interface point (EIP) defined at a radius of 3,522.2 km. A plot of the heliocentric trajectory for the open of the launch period is shown in Figure 1. Also during the Cruise phase, telecom, attitude control, navigation, and lander capabilities to be used during the Entry, Descent, and Landing (EDL) and surface phases will be checked out. The science payload will have a checkout opportunity during the Early Cruise Phase. The spacecraft will require pointing updates to maintain antenna pointing near Earth and the solar panels pointing toward the Sun as their relative positions change during flight.

The Approach sub-phase includes the acquisition and processing of navigation data needed to support the development of the final four trajectory correction maneuvers (TCM-3 through TCM-6), the spacecraft

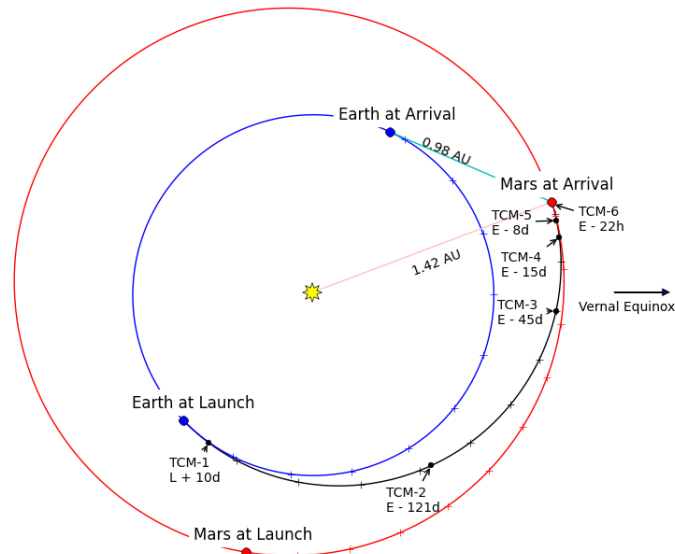


Figure 1. Interplanetary Trajectory for launch on 05/05/2018

activities leading up to separation of the entry vehicle from the cruise stage, and the final turn to the entry attitude. The last four TCMs are used to perform final adjustments to the incoming trajectory at Mars to ensure that the desired entry conditions are achieved. All other spacecraft activities, particularly those that could influence the spacecraft's trajectory (e.g., a spacecraft attitude turn), are minimized. During the Approach sub-phase, the amount of requested DSN tracking is substantially increased to allow more accurate trajectory solutions to be determined in the final weeks before arrival at Mars. In addition to increased Doppler and ranging data, additional Delta Differential One-way Ranging ( $\Delta$ DOR) measurements are also taken during this period to ensure an accurate delivery at Mars.<sup>1,2</sup>

Several days prior to entry, the EDL sequence is loaded on-board the spacecraft and begins executing. This sets a clock running which will bring about the sequence of activities that enable the EDL phase. A final TCM opportunity, along with a contingency TCM during the last 24 hours, may be used to make final corrections to target the Mars atmospheric Entry Interface Point (EIP). Approximately seven minutes before encountering the Martian atmosphere, the Cruise stage is jettisoned from the entry vehicle, and communication via Ultra-High Frequency (UHF) to Earth and to the Mars Reconnaissance Orbiter (MRO) commences. The TCM profile is shown in Table 1.

Event	Location	Date	Objectives
TCM-1	L + 10d	Varies	Removes most of launch vehicle targeting bias and injection errors. TCM-1 includes a deterministic component required to remove the launch vehicle aimpoint bias
Thruster Cal.	E - 153d	Jun 26, 2018	Thruster Calibration induces a small velocity change which is accounted for in TCM-1 design
TCM-2	E - 121d	Jul 28, 2018	Statistical maneuver to correct for orbit determination errors and TCM-1 execution errors; targets to NNIP-biased aimpoint for specific launch date
TCM-3	E - 45d	Oct 12, 2018	Remove remaining aimpoint bias; correct for orbit determination errors, TCM-2 execution errors; targets to EIP for specific launch date
TCM-4	E - 15d	Nov 11, 2018	Statistical maneuver to correct for orbit determination errors and TCM-3 execution errors; targets to EIP for specific launch date
TCM-5	E - 8d	Nov 18, 2018	Statistical maneuver to correct for orbit determination errors and TCM-4 execution errors; targets to EIP for specific launch date
TCM-5X	E - 5d	Nov 21, 2018	Contingency maneuver. Same objectives as TCM-5. Performed only if TCM-5 cannot be executed
TCM-6	E - 22h	Nov 25, 2018 21:40 UTC	Statistical maneuver to correct for orbit determination errors and TCM-5/5X execution errors; targets to EIP for specific launch date
TCM-6X	E - 8h	Nov 26, 2018 11:40 UTC	Contingency maneuver. Final opportunity for entry targeting maneuver. Performed only if TCM-6 does not take place (TCM-6X designed with TCM-6.)
TCM-6XM	E - 8h	Nov 26, 2018 11:40 UTC	Contingency maneuver. Final opportunity for entry targeting maneuver. Will be selected from pre-determined menu of validated maneuvers to maximize the probability of successful landing.
Entry	Entry Interface Point	Nov 26, 2018 19:46:29 UTC to 20:07:29 UTC	Defines the EIP time, entry flight path angle, and B-plane orientation angle at an entry radius of 3522.2 km. Values designed to result in landing at the selected target on the Mars surface

**Table 1. TCM Profile**

### Entry, Descent, and Landing

The entry vehicle then begins its turn to entry attitude six and one-half minutes before entering into the Martian atmosphere. This atmospheric Entry Interface Point is defined to occur at a radius of 3,522.2 km from the center of Mars and represents the point at which atmospheric effects are first expected to be sensed by the spacecraft. Following this direct entry into the Martian atmosphere, the entry vehicle rapidly decelerates due to drag from its hypersonic entry velocities to supersonic parachute deployment velocities as it passes through the increasingly dense atmosphere. The onboard flight software parameters are optimized to guarantee that in the presence of EDL error sources, the chute deployment occurs within the

established Mach/dynamic pressure limits driven by a maximum parachute opening load of 15,000 lbf. The heatshield is jettisoned after the parachute has opened, followed later by the power up of the landing radar and the deployment of the lander legs. The radar will be used during the terminal descent phase to provide input to the descent engines that are then fired to further slow the spacecraft down and land gently on the Martian surface.

Cruise phase navigation and maneuver design will target the E09 ellipse located in the Elysium Planitia region (areocentric latitude = 4.460 deg, East longitude = 135.970 deg) for all launch opportunities. Figure 2 shows the landing ellipse azimuth variation across the launch period. The site has been subjected to extensive reconnaissance by MRO instruments over the years leading to launch.<sup>3</sup>

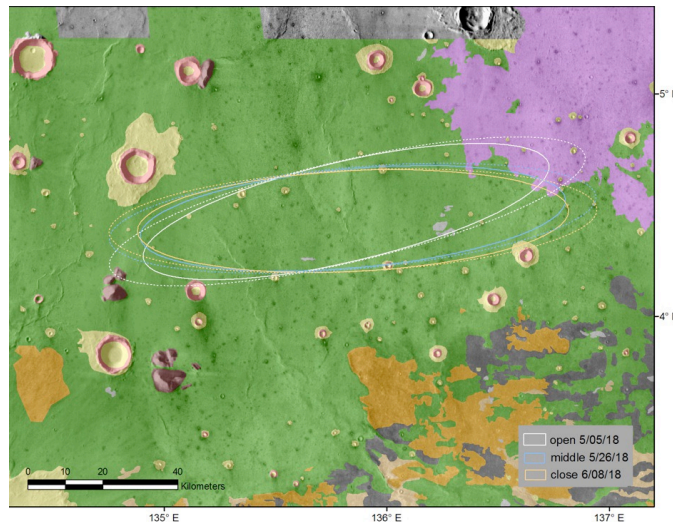


**Figure 2. Landing Ellipse Variation across Launch Period**

## Surface

Once safely on the surface of Mars, the lander is configured for Surface operations. The solar arrays are deployed. Science and engineering data acquired during EDL and during the first hour on the surface will be transmitted to Earth via the lander-to-orbiter UHF-relay link to assess the state of the lander and to ensure that it has achieved a power/thermal safe state. The Instrument Deployment sub-phase commences once it has been determined that the solar arrays are deployed and the lander is in a safe and communicative state. For the first several sols on the surface, the lander and its surrounding environment, including the workspace, are characterized, the payload elements are checked out, the initial weekly Rotation and Interior Structure Experiment (RISE) measurements are acquired, and the critical data collected on Sol 0 – the landing sol – continue to be relayed back to Earth. After the Science team has selected suitable deployment sites within the workspace, the Instrument Deployment Arm places the Seismic Experiment for Interior Structure (SEIS) and Heat Flow and Physical Properties Package (HP<sup>3</sup>) instruments on the Martian surface. Then, with both instruments in their final positions on the surface of Mars, and with SEIS collecting its science data, the HP<sup>3</sup> mole is released. Once the flight team has confirmed that the HP<sup>3</sup> mole has been released, the Penetration sub-phase begins. During this phase, the mole is allowed to penetrate the Martian regolith until it reaches its final depth over the course of about 30 sols. SEIS and HP<sup>3</sup> acquire Science data throughout this phase, and RISE measurements continue to be acquired.<sup>1,2</sup>

The Science Monitoring sub-phase starts at the conclusion of the Penetration sub-phase. SEIS, HP<sup>3</sup>, and RISE continue to collect science data throughout this phase. Science monitoring continues for one Mars year plus 40 sols after landing, with the possibility of extended surface operations continuing for as long as there is adequate power and funding.

## SPACECRAFT

The InSight flight system design is based heavily on the Lockheed Martin-built Phoenix flight system that successfully landed on the surface of Mars in May of 2008. The InSight spacecraft is highly centralized and designed around a core lander that controls all functions throughout all mission phases. Three secondary flight elements (the cruise stage, heatshield, and backshell) provide the additional functions

needed for Cruise and EDL. Figure 3 shows an expanded view of the InSight flight system. The mass allocation for the entire flight system, including propellant, is 700.5 kg.

The InSight lander contains all of the avionics, power electronics, and propulsion system. Most of the Guidance and Navigation Control hardware is located in the lander, augmented during cruise by redundant star trackers and sun sensors mounted on the cruise stage. The majority of the telecommunications hardware is located on the lander, but during cruise an additional X-band transponder and dual amplifiers located on the cruise stage provide redundant X-band communications. The Cruise stage also provides power during cruise via two fixed-wing solar arrays. The backshell and heatshield provide protection for the lander during entry, and the backshell houses the parachute that will slow the entry system prior to terminal descent. Figure 4 shows the flight system in cruise configuration. <sup>1,2</sup>

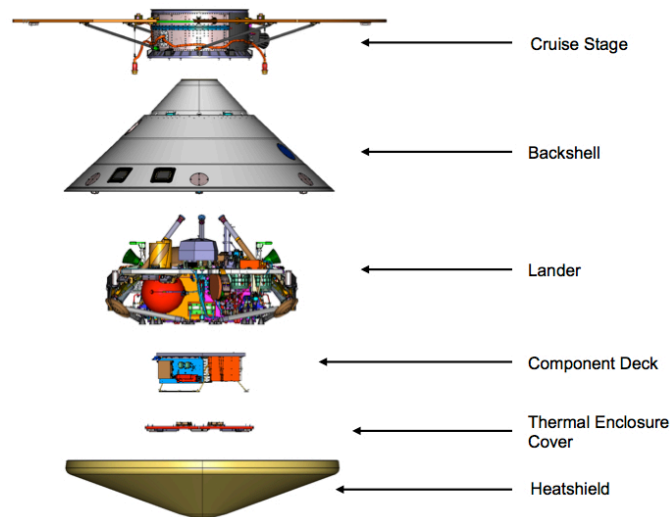


**Figure 3. InSight Flight System – Expanded View**

### **Propulsion System**

The lander propulsion system performs all cruise and EDL propulsion functions. Rocket Engine Modules (REMs) are scarfed through the aeroshell to allow Reaction Control System (RCS) and cruise TCM functions. Specifically, the system consists of four 1-lbf (4.4-N) RCS thrusters to provide attitude control, four 5-lbf (22-N) TCM thrusters to provide  $\Delta V$  maneuvers during cruise, and twelve 68-lbf (302-N) descent engines to allow for EDL deceleration and attitude control. This configuration, including scarf and REM seal designs, was proven through extensive testing and the Phoenix flight. <sup>1,2</sup>

### **Telecom System**

The cruise telecommunications subsystem comprises fully redundant X-band Small Deep-Space Transponders (SDSTs) and Solid-State Power Amplifiers (SSPAs). It provides redundant transmit and receive capability through a fixed, dual-frequency, medium-gain horn and two low-gain patch antennas (one transmit, one receive). To accommodate the radio science experiment (RISE), one of the SDSTs was moved from the Cruise Stage to the Lander and an SSPA was added, both inside the thermal enclosure. Two fixed Medium Gain Antennas (MGAs) provide redundancy during landed operations. During EDL, a UHF transceiver relays critical-event data to MRO and back to Earth. Prior to backshell separation, a wrap-around antenna on the backshell provides coverage, followed by the use of a helix antenna during terminal descent. During landed operations, the UHF transceiver performs relay operations to Mars orbiting assets from the lander twice per day on average. If successful, during EDL the two MarCO spacecraft will provide 8 kbps near real-time bent-pipe communications, although this is not essential to the success of InSight EDL. <sup>1,2</sup>

### **Attitude Control System**

The spacecraft Attitude Control System (ACS) consists of two star trackers, two Miniature Inertial Measurement Units (MIMU), and Sun sensors. The primary attitude determination is done via the star trackers and the MIMU system. The analog Sun sensors serve as a backup system. Unlike the Mars

Science Laboratory (MSL) spinning-stabilized attitude control strategy, the InSight spacecraft is three-axis stabilized via an unbalanced thruster control system. The RCS thrusters are fired intermittently to maintain a pre-determined deadband attitude profile. Additionally, the RCS thrusters are used to maintain attitude during TCMs (roll only) and safe-mode (3-axis control). The TCM  $\Delta V$  and pitch/yaw control are performed by the TCM thrusters.<sup>1,2</sup>

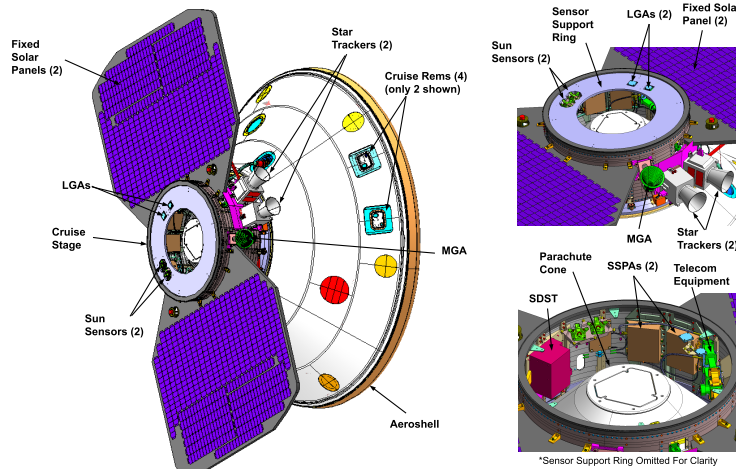


**Figure 4. InSight Flight System – Cruise Configuration**

### Attitude Deadbanding

Since the InSight spacecraft is three-axis stabilized, its attitude is not fixed. The attitude will vary within a set of deadbanding constraints defined by spacecraft telecom, power and thermal subsystems. ACS will command the thrusters to fire each time the attitude reaches one side of the deadband. The deadbands per axis  $[x, y, z]$  are  $[10, 10, 7.5]$  deg before 07/13/18, and are reduced to  $[4, 4, 4]$  deg from 07/13/18 to the slew to Entry.

### Cruise Attitude

The cruise attitude strategy is to maintain the -X-axis pointed between the direction to the Earth and direction to the Sun. This strategy allows a telecom link to Earth using the Low Gain Antenna (LGA) or MGA antenna while providing sufficient power for spacecraft operations. The Cruise phase for InSight is divided into early Cruise and late Cruise. The transition from early to late Cruise will take place on 08/08/18. This transition date is fixed for all launch opportunities. In early Cruise, the LGA is used and the spacecraft attitude is such that the -X-axis face (solar array normal) of the solar arrays is offset 50 deg from the Sun. This is driven by spacecraft thermal constraints. This configuration puts the MGA in the Sun/Earth plane. During this period, the LGA will be used for communications. For late Cruise, communications are switched to the MGA and the spacecraft -X-axis is pointed in the direction of the Sun.

## REQUIREMENTS

The key and driving requirements for mission and navigation design are listed below:

The launch/arrival strategy shall...

### Launch/Arrival Strategy

- ... launch between the dates of May 5 and June 8, 2018 both inclusive.
- ... support a Mars arrival of November 26, 2018.
- ... approach EDL with a V-infinity upper limit of 3.941 km/s.
- ... land in a region bounded by 5°N to 3°N.

### EDL Coverage

- Mission Design and Navigation (MDNAV) shall design a spacecraft trajectory that provides line of sight to the Earth from cruise stage separation to touchdown plus 60 s.

- MDNAV shall design a spacecraft trajectory that has the capability to support UHF-band telecommunications with the Mars Reconnaissance Orbiter from Entry through touchdown plus 60 s.

### TCM $\Delta V$

- MDNAV shall assume that the cumulative  $\Delta V_{99}$  for all Trajectory Correction Maneuvers (TCMs) targeted to the nominal landing site shall not exceed 30 m/s.

### Atmospheric Entry Delivery/Knowledge Accuracies

- The entry vehicle shall approach EDL with an Entry Flight Path Angle (EFPA) of  $-12.0 \text{ deg} \pm 0.21 \text{ deg}$ ,  $3\sigma$ .
- MDNAV shall provide a final update to the entry state (known as the knowledge state) with a  $3\sigma$  Entry Flight Path Angle uncertainty of  $\pm 0.21 \text{ deg}$  and a  $3\sigma$  entry time uncertainty of  $\pm 1.5 \text{ s}$  not later than the last TCM plus 3 hours.
- MDNAV shall design a trajectory that has the capability to land the spacecraft within a 150 km by 35 km ellipse with a probability greater than or equal to 99%.

### Planetary Protection

- The injection aimpoint for launch shall be biased away from Mars such that the probability of the launch vehicle upper stage impacting Mars is less than  $1.0 \times 10^{-4}$  for fifty years after launch.
- The probability of non-nominal impact of Mars due to failure during the cruise phase shall not exceed  $1.0 \times 10^{-2}$ .

## MISSION DESIGN

### Launch/Arrival Strategy

The InSight launch/arrival strategy was designed to provide critical EDL communications via direct-to-Earth (DTE) and the Mars Reconnaissance Orbiter (MRO) using the UHF link for landing sites between  $5^\circ\text{N}$  and  $3^\circ\text{N}$ . The primary constraints in the design of the launch/arrival strategy are the launch vehicle capability, a maximum allowable hyperbolic excess velocity at arrival (VHP) of 3.941 km/s, and a nominal MRO Local Mean Solar Time (LMST) of 3 PM at the time of EDL (note that MRO will be providing EDL communications from a 2:52 PM LMST to further improve performance of the telecom link). The launch/arrival strategy selected is illustrated in Figure 5.

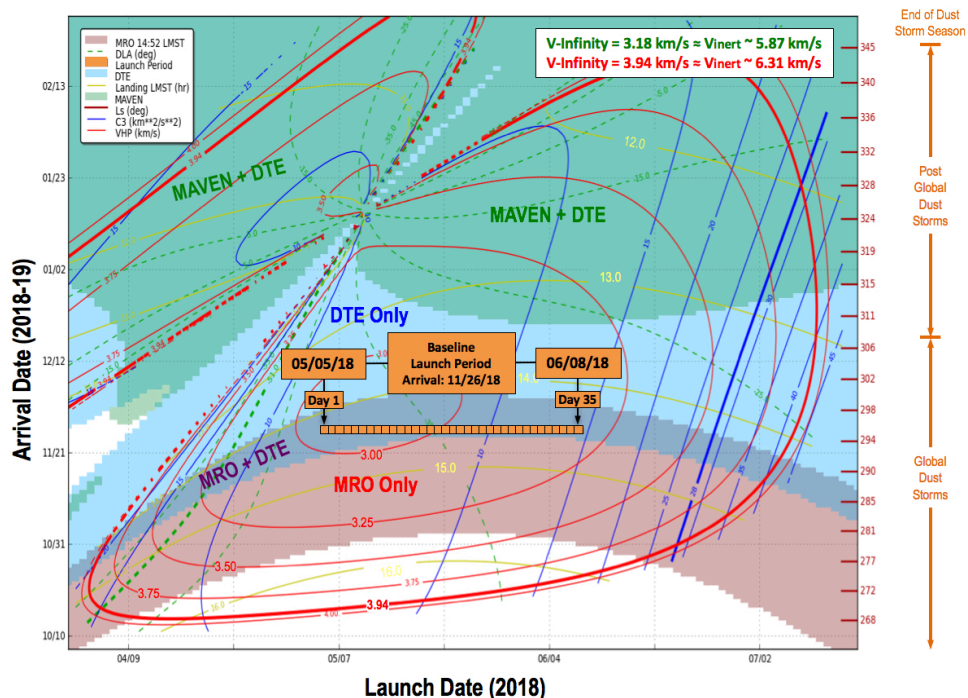


Figure 5. Launch/Arrival Strategy

## Launch Period Characteristics

The launch vehicle targets represent the conditions of the osculating departure at the Targeting Interface Point (TIP) expressed in an Earth-center, inertial, Earth Mean Equator and Equinox of J2000 (EME2000) coordinate system. These Earth-relative target conditions are defined to occur 20 min (1,200 s) after MECO-2 and are shown in Table 2 along with the arrival V-infinity and arrival declination. The launch targets are held constant across the launch window for each day in the launch period and correspond to the optimal launch time for each launch day. The maximum C3 occurs at the close of the launch period, whereas the maximum DLA occurs at the open of the launch period. Note that six launch window cutouts exist through the launch period. Two cutouts on day 1 (05/05) and one on day 2 (05/06) due to late 2<sup>nd</sup> Centaur burn mandatory coverage period violations; one on day 9 (05/13) and one on day 14 (05/18) to preserve margins on injection accuracy; and one on day 11 (05/15) due to injection error requirement violations.

Launch Day	Launch Date (2018, UTC)	Launch Window Duration (min)	Launch Opps	Earth Centered EME2000			IAU Mars Pole	
				C3 (km <sup>2</sup> /s <sup>2</sup> )	DLA (deg)	RLA (deg)	Arrival V-Infinity (km/s)	Arrival Declination (deg)
1	05/05	120	23	8.197	-40.829	328.132	2.978	13.331
2	05/06	120	24	8.063	-40.427	326.878	2.974	12.767
3	05/07	120	25	7.942	-39.899	325.471	2.972	12.233
4	05/08	120	25	7.856	-39.286	324.213	2.970	11.733
5	05/09	120	25	7.795	-38.749	323.070	2.969	11.270
6	05/10	120	25	7.752	-38.274	321.945	2.968	10.836
7	05/11	120	25	7.727	-37.846	320.817	2.969	10.430
8	05/12	120	25	7.720	-37.447	319.683	2.969	10.047
9	05/13	115	24	7.731	-37.069	318.548	2.971	9.685
10	05/14	120	25	7.762	-36.706	317.416	2.973	9.344
11	05/15	115	24	7.813	-36.353	316.297	2.975	9.020
12	05/16	120	25	7.882	-35.958	315.186	2.978	8.711
13	05/17	120	25	7.974	-35.571	314.139	2.982	8.411
14	05/18	115	24	8.085	-35.237	313.071	2.985	8.139
15	05/19	120	25	8.215	-34.863	312.067	2.990	7.872
16	05/20	120	25	8.375	-34.670	311.139	2.995	7.616
17	05/21	120	25	8.543	-34.350	310.231	3.000	7.371
18	05/22	120	25	8.727	-34.036	309.367	3.006	7.136
19	05/23	120	25	8.925	-33.729	308.545	3.012	6.910
20	05/24	120	25	9.138	-33.432	307.765	3.018	6.692
21	05/25	120	25	9.365	-33.143	307.022	3.025	6.482
22	05/26	120	25	9.606	-32.864	306.315	3.033	6.280
23	05/27	120	25	9.851	-32.457	305.563	3.041	6.061
24	05/28	120	25	10.130	-32.334	305.007	3.050	5.895
25	05/29	120	25	10.415	-32.089	304.412	3.059	5.712
26	05/30	120	25	10.719	-31.871	303.869	3.068	5.535
27	05/31	120	25	11.042	-31.743	303.402	3.078	5.365
28	06/01	120	25	11.350	-31.930	302.705	3.088	5.206
29	06/02	120	25	11.651	-31.447	301.593	3.099	5.036
30	06/03	120	25	12.035	-30.998	301.152	3.111	4.871
31	06/04	120	25	12.436	-30.715	300.728	3.123	4.715
32	06/05	120	25	12.856	-30.473	300.297	3.136	4.563
33	06/06	120	25	13.297	-30.247	299.874	3.149	4.416
34	06/07	120	25	13.763	-30.029	299.466	3.163	4.272
35	06/08	120	25	14.255	-29.817	299.079	3.177	4.132

Table 2. Launch Targets and Arrival Characteristics

## EDL Coverage

The selected launch period satisfies the requirement of maintaining full EDL communications from Entry to landing plus 1 min via both MRO and direct-to-Earth. It is assumed that EDL communications are available when the asset (MRO or Earth) has direct line of sight to InSight, i.e., InSight is not occulted by Mars as seen by the asset, and the antenna angle is within the antenna angle constraints. The antenna angle is defined as the angle between the atmosphere-relative anti-velocity vector and the line of sight to the asset. Even though the resulting UHF antenna boresight actually points along the  $-Z$ -axis, 6-DOF simulations indicate that the anti-velocity vector is a valid approximation to the modeling of the  $-Z$ -axis direction during EDL. The antenna angle constraint is 135 deg. It is also required that the elevation angle from landing to landing plus 1 minute is at least 10 deg above the horizon line. Based on these constraints, a range of MRO mean anomalies at Entry Interface Point (EIP) has been identified. This range defines the orbital phasings from which MRO could provide EDL communication services. Given MRO's on-orbit phasing control of  $\pm 30$  s or  $\pm 1.6$  deg, only mean anomaly ranges of at least 5 deg are acceptable. This value includes margin to account for evaluation of EDL communication geometries using conic approximations.<sup>1,2</sup> In order to provide EDL communications coverage for the original landing in 2016, on 07/29/15, MRO performed an inclination change maneuver to allow its ascending node to drift from 3:05 PM LMST through 2:30 PM LMST at the time of EDL. Following cancellation of the 2016 InSight launch, on 04/06/16 (2:44 PM LMST) MRO performed a second maneuver to re-direct its node towards a 3:00 PM LMST. In preparation to support the landing in 2018, MRO executed a third maneuver on 03/22/17 to attain a 2:52 PM LMST at the time of the InSight EDL event. NASA's Mars Odyssey and MAVEN orbiters as well as ESA's Mars Express orbiter have unfavorable geometry with respect to InSight and will not be able to provide EDL communication services. The MarCO technology demonstration known as Mars Cubesat One (MarCO) composed of two 14-kg 6U cubesats will provide EDL communication support in near real-time. Figure 6 illustrates the arrival geometry.

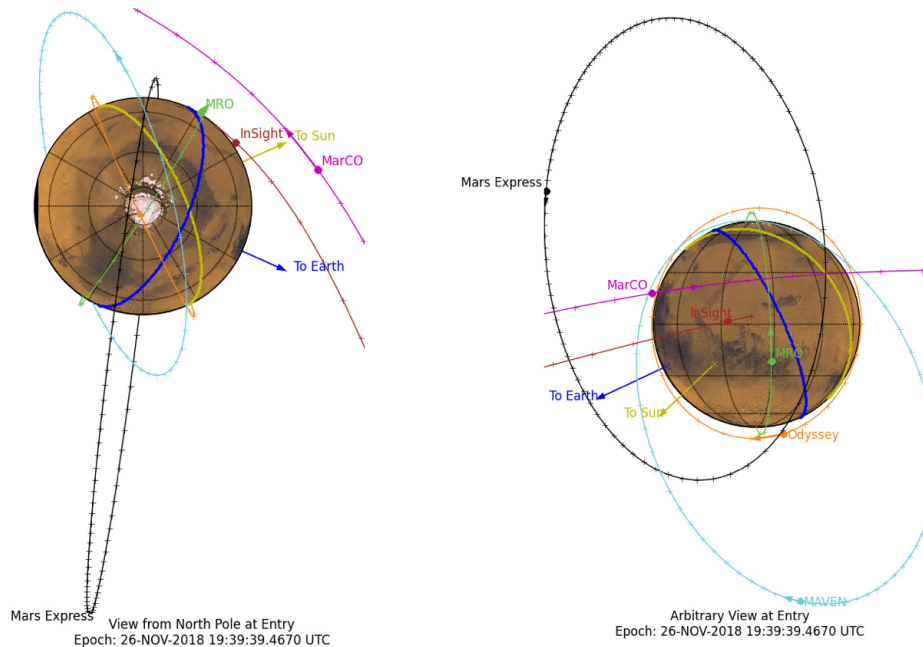


Figure 6. Arrival Geometry

## NAVIGATION

### Tracking Data

The baseline radiometric data types that will be used for InSight orbit determination are two-way coherent Doppler, two-way ranging, and Delta Very Long Baseline Interferometry ( $\Delta$ VLBI) measurements generated by the DSN for an X-band tracking system or a spacecraft to spacecraft UHF system. Doppler and ranging measurements are derived from a coherent radio link between the spacecraft and a receiver at a

DSN ground station.  $\Delta$ VLBI measurements will be acquired through DSN-DSN baselines in the form of Delta Differential One-way Range ( $\Delta$ DOR) measurements. The baseline Doppler, Range, and  $\Delta$ DOR tracking scenarios are shown in Tables 3 and 4. Spacecraft to spacecraft two-way coherent UHF Doppler will be generated by a link between the InSight spacecraft and a Mars orbiting spacecraft during the surface phase.

Relative Dates	Support
Launch to L + 30 days	Continuous 34-m coverage
L + 31 days to E - 141 days	One 34-m 8-hour passes/day*
E - 140 days to E - 119 days	Two 34-m 8-hour passes/day*
E - 118 days to E - 65 days	Five 34-m 8-hour passes/week
E - 64 days to E - 31 days	Two 34-m 8-hour passes/day*
E - 30 days to E - 15 days	Continuous 34-m coverage
E - 15 days to E - 5 days	Continuous 70-m or 34-m redundant
E - 5 days to Entry	Continuous 70-m or 34-m redundant + two 4-hour 35-m NNOR for TCM-6/6X uplink
*Additional 4 days continuous coverage for TCM-2/-3 + Thruster Calibration	

**Table 3. Baseline Doppler and Range Tracking Scenario**

For the navigation analysis reported in this document, the  $\Delta$ DOR observables are assigned a metric data accuracy of 60 ps ( $1-\sigma$ ), and the quasar angular positions are assigned an uncertainty of 1 nrad ( $1-\sigma$ ). A 2-hour latency due to the transmission and processing time required for  $\Delta$ DORs is assumed.

Phase	Dates (UTC)	Stations	Number of $\Delta$ DOR
Pre TCM-3	06/14/18 – 10/12/18	GLD/CAN	21
		GLD/MAD	0
Pre TCM-4	10/13/18 – 11/11/18	GLD/CAN	20
		GLD/MAD	16
Pre TCM-5	11/12/18 – 11/18/18	GLD/CAN	7
		GLD/MAD	7
Approach	11/19/18 – 11/26/18	GLD/CAN	8
		GLD/MAD	8
<b>87 DSN <math>\Delta</math>DOR Passes: Canberra (CAN): 56, Madrid (MAD): 31</b>			

**Table 4. Baseline  $\Delta$ DOR Tracking Scenario**

**Attitude Maintenance Acceleration Uncertainty (Small Forces)**

The small force acceleration uncertainty is the acceleration equivalent of the uncertainty associated with the thrusting involved with attitude maintenance. Each time a thruster is fired to maintain the attitude inside predefined deadbands a small force or  $\Delta$ V is imparted to the trajectory. It is important for the orbit determination (OD) process to model the error associated with these  $\Delta$ Vs. Because the spacecraft design is essentially a reflight of Phoenix, the covariance study has been using the in-flight data from Phoenix to calibrate the uncertainties associated with the small forces. The modeling of the deadbanding uncertainty is based on analysis of these data and is consistent with the following: (1) The bias in all directions is estimated and propagated as a prediction for future deadbanding, (2) the *a priori* uncertainty is set to  $2.0e-11$  km/s<sup>2</sup>, although it should be noted that the post-fit uncertainty in this term is greatly reduced with OD filtering and is not a significant source of error for prediction, and (3) the variations about the mean, as seen in the Phoenix data, are modeled with two different stochastic acceleration models.<sup>1,2</sup>

- First, a white noise bias term is used to account for the short-term pulse to pulse variations and the timing and number of actual thruster pulses in the future compared to the prediction. This term has been set to an *a priori*  $\sigma$  value of  $2.25e-11$  km/s<sup>2</sup> for the spacecraft X-direction and  $4.5e-12$  km/s<sup>2</sup> for spacecraft Y- and Z-directions.
- Long term effects observed in the data are modeled as a correlated noise process with a time constant of 14 days. The *a priori* uncertainty for those is  $7.4e-12$  km/s<sup>2</sup> in the spacecraft X-direction and  $1.5e-12$  km/s<sup>2</sup> in the spacecraft Y- and Z-directions.

### Filter Configuration and Assumptions

The major error sources in orbit determination are TCM uncertainty and  $\Delta$ DOR accuracy. The OD filter assumptions and error sources for the orbit determination results are shown in Table 5. In this table, “Est” indicates parameter estimation, “Stoch” indicates estimation with stochastics, and “Con” indicates consider covariance.

Error Source	Estimate	Uncertainties ( $1\sigma$ )			Comments
		Baseline	Degraded	No Margin	
2-way Doppler weight (mm/s)	-	0.1	0.2	0.05	
Range weight (m)	-	3	6	3	
DSN GLD/CAN $\Delta$ DOR weight (ps)	-	60	120	60	
DSN GLD/MAD $\Delta$ DOR weight (ps)	-	60	120	60	
DSN $\Delta$ DOR latency (hr)	-	2	17	2	
TCM and TCM Slews	Est	1.0 x Req	1.2 x Req.	0.8 x Req.	
Thruster Frame Y Direction (deg)	Est	3	3 deg bias + stoch 3 deg	1	1 day update, 0 correlation, Deadband white.
Thruster Frame Z Direction (deg)	Est	3	3 deg bias + stoch 3 deg	1	1 day update, 0 correlation, Deadband white.
Thruster Acceleration Magnitude Scale (%)	Stoch	3% bias, 5% stoch	3% bias, 15% stoch	1% bias, 5% stoch	1 day update, 0 correlation, Deadband white. Post-arc sigma = 15%
Solar Pressure Scale Factor (%)	Stoch + Bias	Stoch = 3, Bias = 10	Stoch = 10, Bias = 10	Stoch = 3, Bias = 10	1 day update, 7-day correlation, SRP ecrv
Range Bias (m)	Stoch	2	4	1	1 year update, 0 correlation, Range bias white
Day Ionosphere (cm)	Con	55	75	27.5	
Night Ionosphere (cm)	Con	15	30	7.5	
Wet Troposphere (cm)	Con	1	2	0.25	
Dry Troposphere (cm)	Con	1	2	0.25	
X/Y Pole (cm)	Con	1	2	1	
UT1 (cm)	Con	2	4	2	
Station Locations	Con	2003 Cov	2003 Cov	2003 Cov	
Quasar Locations (nrad)	Con	1	2	0.5	
Mars GM (km <sup>3</sup> /s <sup>2</sup> )	Con	2.80E-04	2.80E-04	2.80E-04	
Earth-Mars Ephemeris scale	Con	1.0 x	2 x	0.5 x	
Earth GM (km <sup>3</sup> /s <sup>2</sup> )	Con	1.40E-03	1.40E-03	1.40E-03	
Moon GM (km <sup>3</sup> /s <sup>2</sup> )	Con	1.00E-04	1.00E-04	1.00E-04	
Deimos, Phobos Ephemeris	Con	1.0 x	1.0 x	1.0 x	

**Table 5. Covariance Analysis Filter Assumptions**

## Cruise/Approach Navigation Accuracies

The orbit determination results presented in this section are based on the use of Doppler, range, and  $\Delta$ DOR tracking data. They represent mappings of spacecraft state knowledge. The state uncertainty at the OD data cutoff (DCO) for each TCM design is mapped from the data cutoff time to the Mars-centered, Mars Mean Equator of Date B-plane at the time of Entry.

The OD data cutoffs for TCMs -1, -2, and -3 are 5 days before the respective maneuver. The OD data cutoffs for TCMs -4, -5 and -6 are 24 hours before the burns. The OD data arc used to compute the covariance for a given TCM design, depending on the circumstances, may or may not include the preceding TCM. The data arc for TCM-3 starts after TCM-2 and does not include TCMs -1 or -2. The data arcs for the approach TCMs -4, -5, and -6 start prior to TCM-3 at 60 days before entry. TCM-6X would be attempted if, for whatever reason, TCM-6 could not be executed, and this maneuver was required to ensure that the atmospheric entry delivery accuracy requirements are met. Similarly, TCM-6XM would be executed if the additional tracking data following TCM-6/6X DCO indicated that the delivery accuracy requirements could not be met. Note that TCM-6X and TCM-6XM have the same execution time.<sup>1,2</sup>

Figure 7 shows the associated mapping history of the entry flight path angle (EFPA) uncertainties with respect to DCOs. As seen in this figure, the EFPA uncertainties meet the requirement about four days before the TCM-6 data cutoff. B-plane error ellipses resulting from the TCM-5 delivery, TCM-6 delivery and the corresponding knowledge statistics for the open, middle, and close of the launch period targeted to the E09 landing site for the baseline scenario are shown in Figures 8 through 10. The InSight B-plane delivery error ellipse is nearly circular due to the dominance of the TCM slew errors. A nearly circular B-plane error ellipse minimizes the B-plane angle's effect on the EFPA dispersion. As demonstrated in these figures, the EFPA uncertainties meet the requirement about four days before the TCM-6 data cutoff.

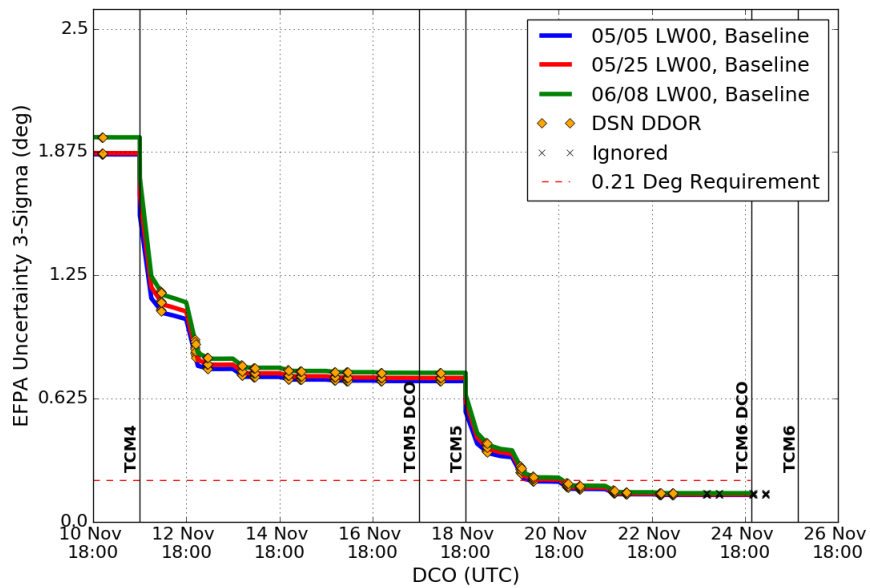
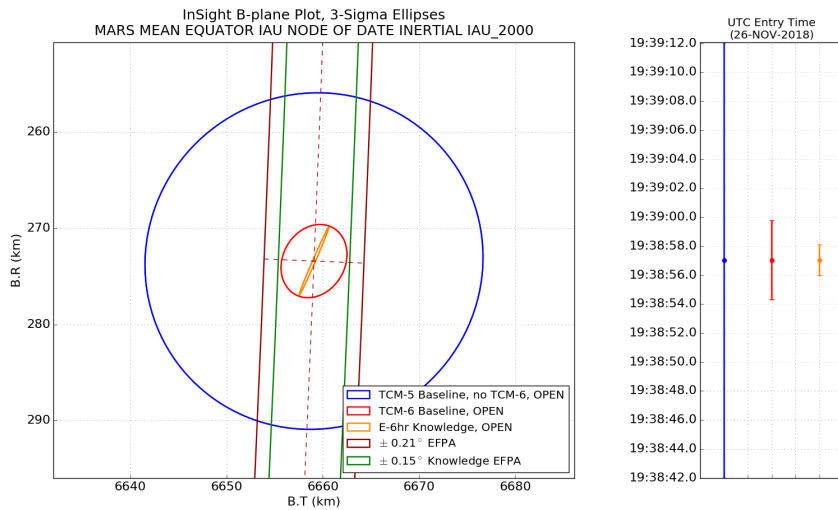
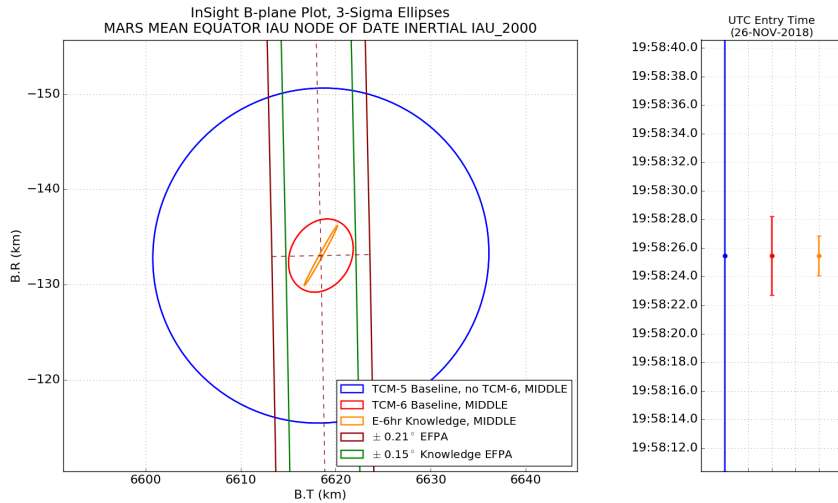


Figure 7. Evolution of EFPA Uncertainty with respect to DCO (Baseline)



**Figure 8. TCM-5 Delivery, TCM-6 Delivery/Knowledge B-plane Error Ellipse, and Entry Time Uncertainty (Baseline, Open)**



**Figure 9. TCM-5 Delivery, TCM-6 Delivery/Knowledge B-plane Error Ellipse, and Entry Time Uncertainty (Baseline, Middle)**

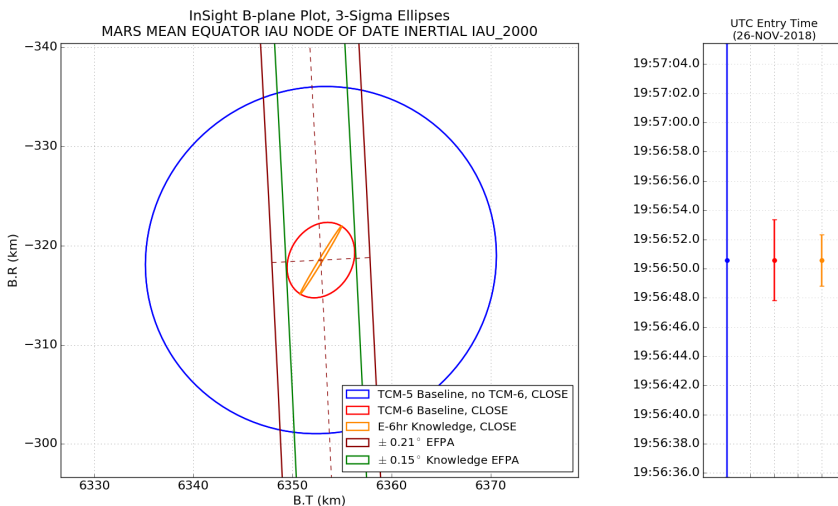


**Figure 10. TCM-5 Delivery, TCM-6 Delivery/Knowledge B-plane Error Ellipse, and Entry Time Uncertainty (Baseline, Close)**

## Sensitivity to Filter Assumptions

A series of parameterized sensitivity cases for the Approach phase were analyzed in order to determine the effects of changes to data assumptions and modeling uncertainties on the delivery accuracy for TCM-6 EFPA. The “No Margin” case represents an optimistic scenario with the following assumptions: (1) actual performance is on par with prior mission experience rather than at the level of the requirements, (2) all requested Doppler and range tracking passes are successful, and (3) all requested  $\Delta$ DOR measurements are successful and delivered within the expected timeframe. The difference in results between the “No Margin” and the baseline cases quantifies the amount of margin included in the navigation design. Table 5 includes the nominal assumptions labeled as “Baseline”, a degraded uncertainty for each parameter studied labeled as “Degraded” and an improvement over the baseline for each parameter studied labeled as “No Margin”. Figure 11 illustrates the history mapping of these three filter scenarios.

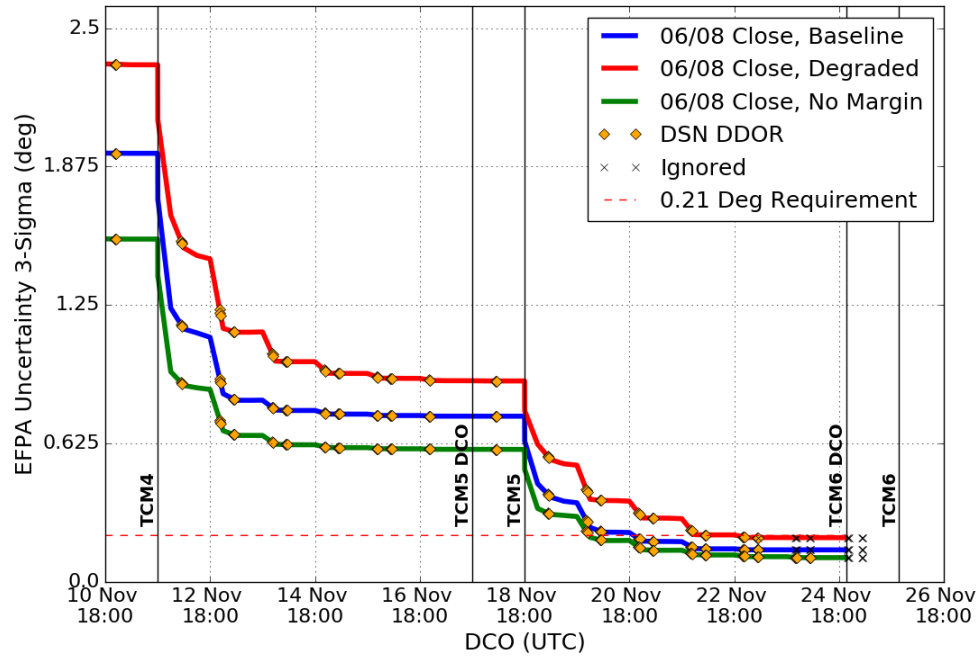


**Figure 11. Baseline/No Margin/Degraded History Mapping**

All three scenarios meet the EFPA requirement of 0.21 deg ( $3\text{-}\sigma$ ) with varying margin. Both “Baseline” and “No Margin” cases easily satisfy the EFPA requirement with 31% and 48% margin, respectively. The “Degraded”  $3\text{-}\sigma$  EFPA uncertainty is 0.20 deg which marginally still meets the requirement.

Figures 12 and 13 show the EFPA history and associated B-plane error ellipses with respect to the Entry requirement. As illustrated in Figure 12, Goldstone-Madrid  $\Delta$ DOR measurements are critical to meet the EFPA uncertainty. The launch opportunity at the close of the launch period, 06/08/18, corresponds to the largest EFPA uncertainty and is therefore shown in Figure 13 since it is the most stressing case.

Figure 14 shows the baseline delivery EFPA solution uncertainty for open, middle, and close of each launch opportunity; there is very little variation across both launch window and launch period.

In conclusion, the delivery and OD accuracies are well behaved and sensitive to typical parameters such as dynamic uncertainties and data accuracy. The most significant sensitivities are caused by changes in TCM slew uncertainties and  $\Delta$ DOR accuracy and latency. These results support the need for a robust understanding of the spacecraft GN&C uncertainties, a thruster calibration and a highly reliable  $\Delta$ DOR system.

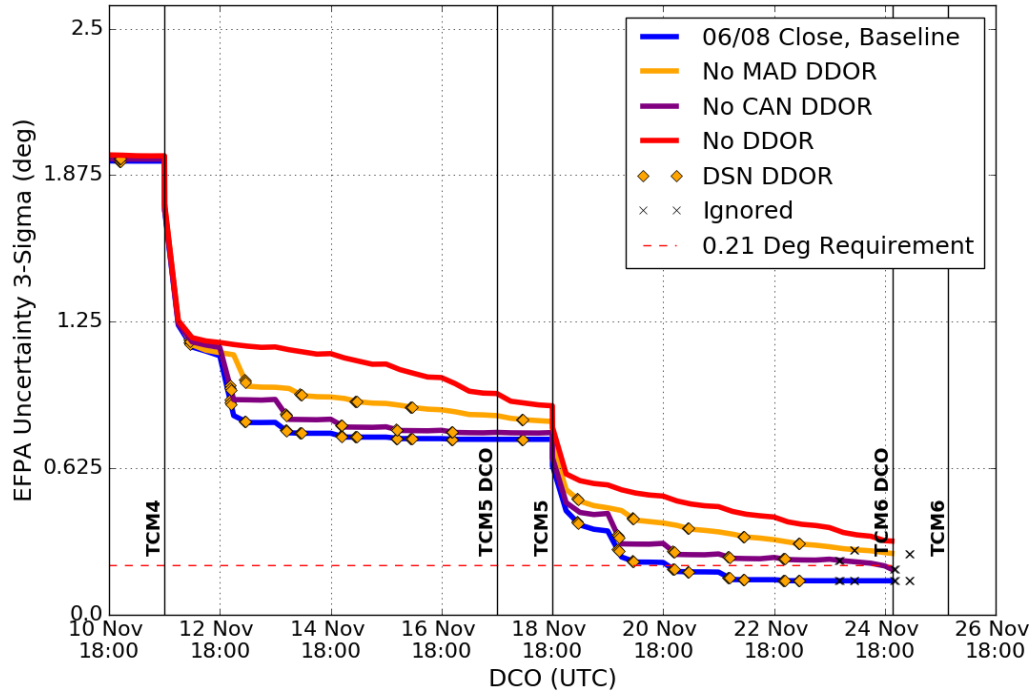


Figure 12.  $\Delta$ DOR Sensitivity (EFPA)

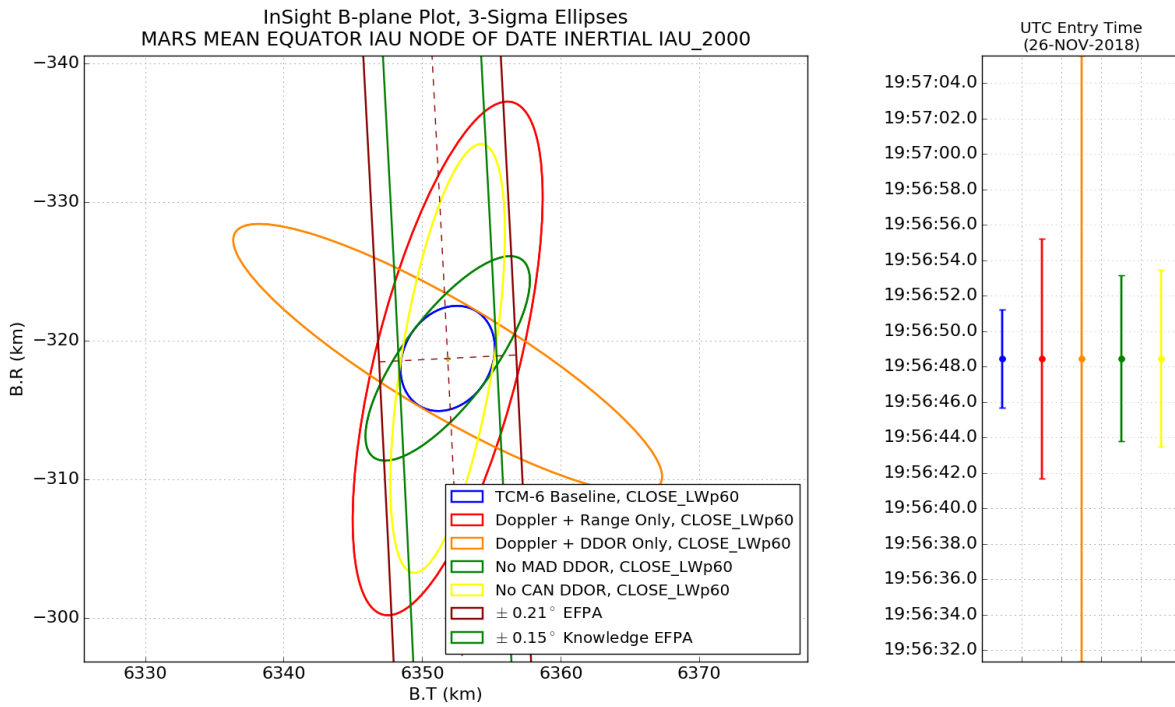
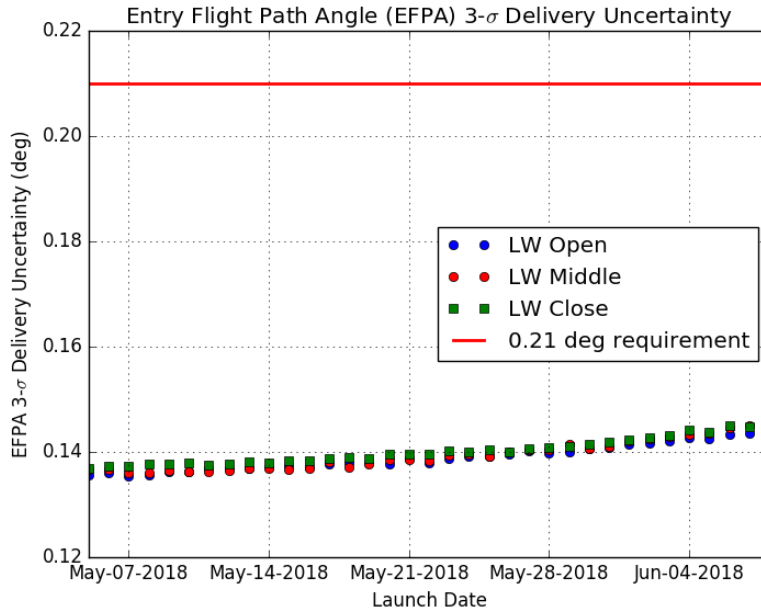


Figure 13.  $\Delta$ DOR Sensitivity (B-Plane)



**Figure 14. Baseline Delivery EFPA Uncertainty across the Launch Period**

**Trajectory Correction Maneuvers**

InSight has scheduled six TCMs, while providing for back-up opportunities for TCMs 5 and 6. Mission  $\Delta V$  requirements for these TCMs are estimated for each launch date by performing 5,000-sample Monte Carlo linear error analyses that model errors due to launch vehicle injection, orbit determination, and maneuver execution. The maneuver execution errors reflect the entire turn-burn-turn process as described in Table 7.

Delta-V Magnitude		Fixed Magnitude Error	Proportional Pointing Error	Fixed Pointing Error	Proportional Pointing Error, Total
Min	Max				
m/s	m/s	m/s	%	m/s per axis	%
0.04	0.3	0.02	2%	0.003	2
0.3	1.5	0.02	2%	0.003	$(8/1.2* dV )$
1.5	5	0.02	2%	0.003	10
5	20	*	2%	0.003	$((-8/15)* dV +12.667)$
$\geq 20$	*	*	2%	0.003	2

**Table 7. Turn-Burn-Turn (1- $\sigma$ ) Maneuver Execution Errors**

Launch vehicle targets are based on optimal performance for each launch day and are fixed during each daily launch window. Table 8 summarizes the total TCM  $\Delta V$  which includes deterministic, statistical and implementation costs at the 99%-tile level for the open of the launch period. This table shows the effects on  $\Delta V$  estimates when launch occurs  $\pm 60$  min with respect to the optimal location. For each case, the cost of TCM-1 is the dominant contributor. Figure 15 shows the mission  $\Delta V_{99}$  for all days in the launch period. The case with the largest mission  $\Delta V_{99}$  of 22.3 m/s occurs at the open of the daily window on 05/27/18. This date has the largest aimpoint bias.

TCM Schedule			TCM $\Delta V$ Statistics (m/s)						
TCM Relative Time	TCM Epoch (2018, UTC)	OD Data Cutoff	Launch Window	Determ. $\Delta V$	Mean $\Delta V$	1 $\sigma$ $\Delta V$	$\Delta V_{01}$	$\Delta V_{99}$	Cumul. $\Delta V_{99}$
TCM-1 L + 10d	May 15, 18:00 (Tue, PDT)	TCM - 5d	Opt-60m	5.021	7.101	2.394	4.661	15.524	15.524
			Optimal	3.588	4.643	1.236	3.028	8.963	8.963
			Opt+60m	3.125	5.867	2.855	2.443	15.256	15.256
TCAL E - 153d	Jun 26 (Tue, PDT)	N/A	Opt-60m	0.472	0.472	0.031	0.400	0.543	16.008
			Optimal	0.472	0.472	0.031	0.400	0.546	9.437
			Opt+60m	0.472	0.472	0.031	0.402	0.543	15.718
TCM-2 E - 121d	Jul 28, 18:00 (Sat, PDT)	TCM - 5d	Opt-60m		0.404	0.262	0.051	1.209	16.605
			Optimal		0.291	0.192	0.881	9.821	
			Opt+60m		0.298	0.220	1.070	16.306	
TCM-3 E - 45d	Oct 12, 18:00 (Fri, PDT)	TCM - 5d	Opt-60m	0.046	0.074	0.038		0.167	16.648
			Optimal	0.046	0.072	0.038	0.166	9.915	
			Opt+60m	0.046	0.073	0.039	0.171	16.387	
TCM-4 E - 15d	Nov 11, 18:00 (Sun, PDT)	TCM - 1d	Opt-60m		0.057	0.038		0.133	16.680
			Optimal		0.058	0.038	0.134	9.962	
			Opt+60m		0.057	0.038	0.135	16.415	
TCM-5 E - 8d	Nov 18, 18:00 (Sun, PDT)	TCM - 1d	Opt-60m		0.027	0.031		0.087	16.717
			Optimal		0.027	0.031	0.087	9.983	
			Opt+60m		0.027	0.031	0.087	16.456	
TCM-6 E - 22h	Nov 25, 21:39 (Sun, PDT)	TCM - 1 d	Opt-60m		0.206	0.083	0.034	0.371	16.827
			Optimal		0.207	0.083	0.033	0.372	10.185
			Opt+60m		0.206	0.083	0.370	16.653	
TOTAL $\Delta V$ :			Opt-60m	5.539	8.341	2.462	5.703	16.827	
			Optimal	4.106	5.770	1.289	4.019	10.185	
			Opt+60m	3.643	7.001	2.951	3.424	16.653	

Table 8. TCM  $\Delta V$  Statistics for Launch Period Open (05/05/18)

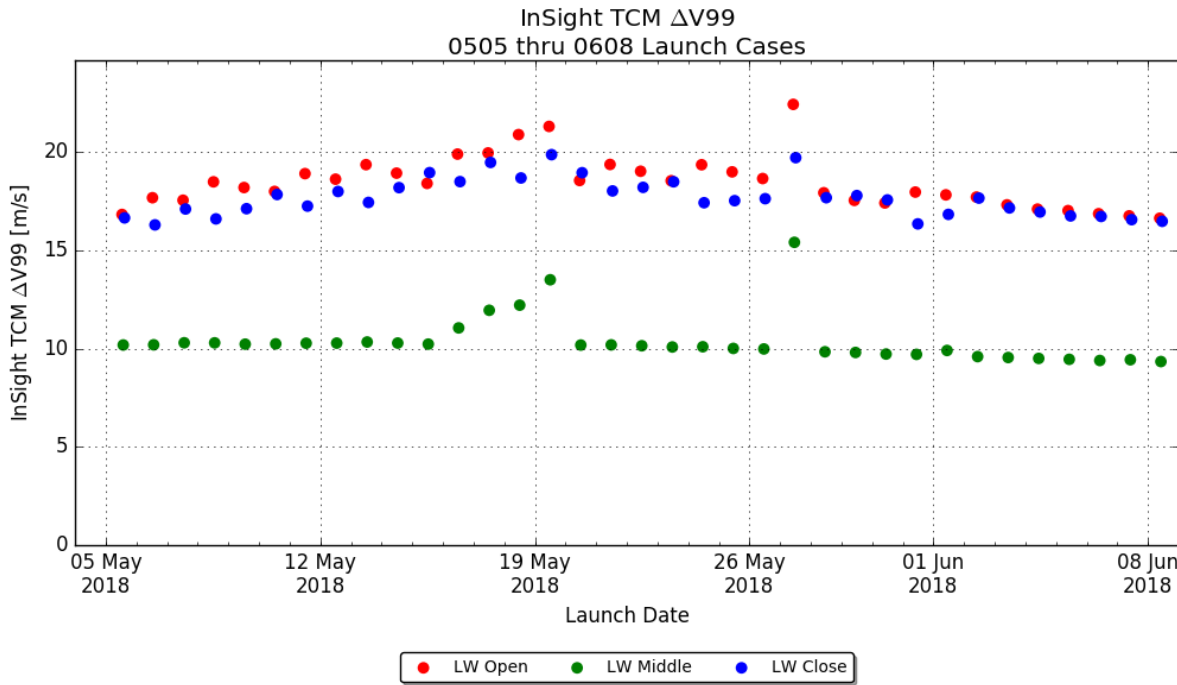


Figure 15. TCM  $\Delta V_{99}$  Distribution across the Launch Period

## 50-Year Planetary Protection

The 99<sup>th</sup> percentile probability of impact for the baseline mission (both MarCOs deploy) and for the two anomalous missions, where one or two MarCOs fail to deploy for the open, middle, and close of the launch window for every day in the launch period are shown in Figure 16. The  $0.69 \times 10^{-4}$  “floor” in these estimates is driven by the number of samples drawn during the Monte Carlo Analyses.<sup>4</sup> The worst-case probability of impact for the baseline scenario is  $0.72 \times 10^{-4}$  and occurs at the open of the launch window for a launch on 05/20/18. The worst-case probability of impact for a one-MarCO deployment scenario is  $0.72 \times 10^{-4}$ . This occurs at the open of the launch window for a 05/10/18 launch. The worst-case probability of impact for a no-MarCO deployment scenario is  $0.71 \times 10^{-4}$ . This occurs at the open of the launch window on 05/15/18.

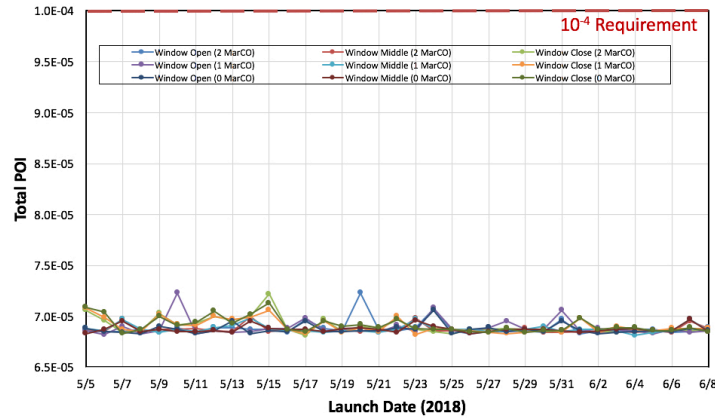


Figure 16. Total Probability of Impact

## Non-Nominal Impact Probability

A non-nominal impact is defined as an impact that could result in the break-up of the spacecraft and release of terrestrial contaminants on Mars. Overall, non-nominal impact probability is the cumulative sum of the probability of non-nominal impact following each TCM. Table 9 shows the cumulative non-nominal impact probability for the open, middle, and close of the launch period. For each launch date, TCMs -1, -2, and -3 are the major contributors to non-nominal impact probability, driven by the larger  $Q(i+1)$  values that reflect the longer times between TCMs early in the mission. The cumulative probability of non-nominal impact satisfies the requirement of  $1.0 \times 10^{-2}$  for each launch date.

Event	Location	Launch 05/05/18			Launch 05/22/18			Launch 06/08/18		
		P(i)	Q(i+1)	P(i)*Q(i+1)	P(i)	Q(i+1)	P(i)*Q(i+1)	P(i)	Q(i+1)	P(i)*Q(i+1)
<b>Launch</b>		0	4.88E-06	0	0	4.79E-06	0	0	4.82E-06	0
<b>Injection</b>		1.00E-04	7.12E-04	7.12E-08	1.00E-04	7.18E-04	7.18E-08	1.00E-04	7.23E-04	7.23E-08
<b>TCM-1</b>	L+10d	0.931	2.94E-03	2.74E-03	0.999	1.75E-03	1.75E-03	0.999	5.66E-04	5.66E-04
<b>TCAL</b>	E-153d	0.488	2.23E-03	1.09E-03	0.480	2.23E-03	1.07E-03	0.474	2.23E-03	1.06E-03
<b>TCM-2</b>	E-121d	0.366	5.31E-03	1.94E-03	0.357	5.31E-03	1.89E-03	0.352	5.31E-03	1.87E-03
<b>TCM-3</b>	E-45d	0.987	2.10E-03	2.07E-03	0.987	2.10E-03	2.07E-03	0.984	2.10E-03	2.06E-03
<b>TCM-4</b>	E-15d	1.000	4.90E-04	4.90E-04	1.000	4.90E-04	4.90E-04	1.000	4.90E-04	4.90E-04
<b>TCM-5</b>	E-8d	1.000	5.01E-04	5.01E-04	1.000	5.02E-04	5.02E-04	1.000	5.02E-04	5.02E-04
<b>TCM-6</b>	E-22h	2.70E-03	6.42E-05	1.73E-07	2.70E-03	6.41E-05	1.73E-07	2.70E-03	6.42E-05	1.73E-07
<b>Cumulative Total:</b>			8.83E-03		<b>Total:</b>	7.78E-03		<b>Total:</b>	6.55E-03	

P(i) : probability of impact after maneuver i  
 = total impact probability (100 km atmosphere) for all maneuvers except TCM-6  
 = probability of impact for non-nominal entry flight path angles for TCM-6  
 Q(i+1) : probability of not being able to execute maneuver i+1 given that maneuver i has occurred.

Table 9. Probability of Non-Nominal Impact for Optimal Launch times

## LANDING ELLIPSE SIZE

Two methods and several atmospheres were used to calculate the 99% ellipse size: (1) A Contour method that contains exactly 99% of the landing points, and (2) a Gaussian method which assumes that all landing points are Gaussian-distributed along each axis. The advantage of the Contour method is that requires no assumptions about the probability of the distribution of landing points; however, it is sensitive to the sample size (the ellipse size can vary significantly for a “small” number of landing points). The Gaussian method is typically well behaved; however, the 99% of the Gaussian ellipse may not contain 99% of the landing points. The landing footprint size for the open, middle, and close of the launch period is shown in Table 11.

Launch Date (2018)	Atmosphere	Azimuth (deg)	Contour Method		Gaussian Method	
			99% Along-track* (km)	99% Cross-track** (km)	99% Along-track* (km)	99% Cross-track** (km)
05/05	Background	76.2	121.8 km	26.5 km	114.3 km	24.9 km
	Global	75.9	129.6 km	27.5 km	119.6 km	25.4 km
06/08	Background	86.8	124.8 km	26.7 km	118.2 km	25.2 km
	Global	86.6	131.4 km	28.1 km	123.1 km	26.4 km

\*Along-track variability:  $\pm 4.7$  km  $3\sigma$  (Contour),  $\pm 3.0$  km  $3\sigma$  (Gaussian)

\*\*Cross-track variability:  $\pm 1.0$  km  $3\sigma$  (Contour),  $\pm 0.6$  km  $3\sigma$  (Gaussian)

**Table 11. Landing Footprint Size**

## CONCLUSIONS

This paper has summarized the launch/arrival strategies, the Navigation and Maneuver Design, and presented results to demonstrate that all InSight Mission Design and Navigation requirements for the 2018 launch are satisfied. This strategy consists of a 35-day launch period that provides EDL communications via UHF to MRO or Direct-To-Earth. Six trajectory correction maneuvers (TCMs) are planned in order to achieve the required entry delivery accuracies.

## ACKNOWLEDGMENTS

The research described in this paper was carried out at the Jet Propulsion Laboratory, California Institute of Technology, under a contract with the National Aeronautics and Space Administration. The author would like to acknowledge the members of the InSight Team who contributed to the analyses that are reported on in this paper: Gene Bonfiglio, Rob Grover, and Matt Golombek. The author also acknowledges the contributions of the GNC team at Lockheed Martin. Roby Wilson served as a reviewer for this paper and provided useful comments. © 2018 California Institute of Technology. Government sponsorship acknowledged.

## REFERENCES

- <sup>1</sup> F. Abilleira, R. Frauenholz, K. Fujii, M. Wallace, T.H. You, “2016 InSight Mission Design and Navigation”, 24<sup>th</sup> AAS/AIAA Space Flight Mechanics Meeting, Santa Fe, New Mexico, January 26-30, 2014.
- <sup>2</sup> F. Abilleira, A. Halsell, K. Fujii, E. Gustafson, C. Helfrich, E. Lau, J. Lee, N. Mottinger, J. Seubert, E. Sklyanskiy, M. Wallace, J. Williams, “Final Mission and Navigation Design for the 2016 Mars InSight Mission”, 26<sup>th</sup> AAS/AIAA Space Flight Mechanics Meeting, Napa, California, February 14-18, 2016.
- <sup>3</sup> M. Golombek, L. Redmond, H. Gengl, C. Schwartz, N. Warner, B. Banerdt, S. Smrekar, “Selection of the InSight Landing Site: Constraints, Plans, and Progress”, 44<sup>th</sup> Lunar and Planetary Science Conference (2013), The Woodlands, Texas, March 18-22, 2013.
- <sup>4</sup> M. Wallace, “Massively Parallel Bayesian Approach to Planetary Protection Trajectory Analysis and Design”, 2015 AAS/AIAA Astrodynamics Specialists Conference, Vail, Colorado, August 9-13, 2015.